ORNL/TM-8132
Dist. Category UC-20g

Contract No. W-7405-eng-26

ORNL/TM--8132

DE82 008903

FUSION ENERGY DIVISION

UNIVERSAL MODE WITH DIFFUSIVE ELECTRONS: LINEAR INSTABILITY AND NONLINEAR SATURATION

C. O. Beasley, Jr.

Fusion Energy Division

K. Molvig

Massachusetts Institute of Technology

W. van Rij

Computer Sciences

Date Published - March 1982

Prepared by the
OAK RIDGE NATIONAL LABORATORY
Oak Ridge, Tennessee 37830
operated by
UNION CARBIDE CORPORATION
for the
DEPARTMENT OF ENERGY

TABLE OF CONTENTS

ABSTRACT

The effect of spatial electron diffusion on the stability properties of the universal drift mode in a sheared magnetic field are studied using an initial value code, TEDIT. Previous studies of this problem by Hirshman and Molvig relied on an approximation to the electron resonance function equivalent to making a Krook approximation for the spatial diffusion operator, $D\,\partial^2/\partial x^2$. The present work treats the diffusion operator precisely and also allows the treatment of a realistic parallel velocity dependence of the diffusion coefficient, $D = D(v_\parallel)$. For the case of a velocity independent diffusion coefficient, the qualitative features found by Hirshman and Molvig are observed. The modes with $k_y\rho_i > 1$ destabilize at small values of the diffusion coefficient and saturate at higher values, corresponding to several orders of magnitude in D. There are quantitative discrepancies with the previous work that, near the saturation point, can be accounted for reasonably well by a simple asymptotic theory. However, when the code uses a more realistic form, $D = D_o\,(v_e/|v_\parallel|) \times \exp(-v_c^2/v_\parallel^2) + D_c$, where D_c corresponds to the (small) collisional diffusion, and D_o parametrizes the turbulence level, then a quantitative difference is observed. Instability persists down to zero turbulence levels, $D_o = 0$. This is essentially linear instability due to collisional diffusion alone.

I. INTRODUCTION

Recent theoretical studies of turbulence associated with universal modes in sheared magnetic fields have led both to encouraging results in the development of a self-consistent theory of universal mode turbulence and to scalings which show reasonable points of agreement with experimentally observed anomalous transport in tokamaks.[1,2] As discussed in this earlier work, the basic physical mechanism responsible for destabilization of a universal mode is the radial diffusion of electron orbits. This diffusion arises physically from either collisions or intrinsic orbital stochasticity of the Chirikov[3] type.

Since a quantitative description of such a phenomenon is inherently dependent on the nature of the nonlinear diffusion of the electron orbits and since the earlier work [1,2] is based on only the simplest models of this diffusion operator, a more rigorous treatment of this operator is needed. In addition, earlier treatments have not included additional important effects like the electron and ion temperature gradient.

An initial value code, TEDIT, capable of calculating radial eigenmodes in the vicinity of a mode-rational surface in a tokamak, had been developed[4] earlier. Because of the inherent simplicity of the electron kinetic equation in this numerical model (described below), inclusion of a physically realistic diffusion operator is straightforward and in no way complicates the calculation of eigenmodes. Indeed, the main virtue of this initial value approach is the flexibility it allows in dealing with this operator, the coefficient of which can include $v_{\parallel}$ dependence. This is noteworthy because the inclusion of such operators in shooting codes (such as used in Refs. 1 and 2) is intractable, except possibly in some simple limits such as that of a constant diffusion coefficient. In particular, the earlier work[1,2] used a Krook-type approximation for this diffusion operator. The effect of this approximate operator on the wave-particle resonance is considerably different from that of a

real diffusion operator, even though qualitatively the effects on the eigenmode may be similar. In addition, inclusion of the electron temperature gradient is straightforward. Although the method is applicable to finite beta, this paper will be concerned mainly with understanding the difference between Krook-type approximation results and diffusion operator results, and in examining the role of electron temperature gradients.

The qualitative features described in Ref. 1 are confirmed. Quantitative discrepancies are observed, but can be explained, near the saturation point, by a simple asymptotic theory. Extending the calculation numerically to include a realistic parallel velocity dependence and collisional diffusion in D shows that the unstable range can extend down to zero turbulence levels.

II. PARTICLE DYNAMICS AND TEDIT CODE DESCRIPTION

The TEDIT model code[4] is an initial value code that follows the time evolution of all perturbed quantities as described below. One begins with an arbitrary perturbed ϕ, f_e, and f_i. Regardless of the initial functions, if a growing (unstable) eigenmode exists, it will eventually dominate the long time solution. By definition, an eigenmode exists when all quantities ϕ, f_e, and f_i vary as $e^{-i\omega t}$, where the eigenfrequency ω is the same for all x.

Both electrons and ions are described kinetically in the TEDIT model. The equations are written in a slab geometry ($x \equiv r$) and are described here in their zero beta limit. The drift-kinetic equation for the perturbed electron distribution function is

$$\left(\frac{\partial}{\partial t} + ik_{\parallel}' x v_{\parallel} - D\frac{\partial^2}{\partial x^2}\right) f_e \qquad (1)$$

$$= -i\frac{e}{T_e} F_e\{\omega_*[1 + \eta_e(\frac{v_\parallel^2}{v_e^2} - \frac{1}{2})] - k'_\parallel x v_\parallel - iD\frac{\partial^2}{\partial x^2}\}\phi \ .$$

F_e and f_e are the unperturbed and perturbed electron distributions gyroaveraged and integrated over $v_\perp$, respectively, ϕ is the perturbed electrostatic potential, and

$$k'_\parallel = \frac{k_y}{L_s}, \ \omega_* = \frac{v_e^2 k_y}{2\Omega_e L_n} \ , \ v_e = \sqrt{\frac{2T_e}{m_e}} \ , \ \eta_e = \frac{d\ (\ln T_e)}{d\ (\ln n_o)},$$

where k_y is the poloidal wave number, L_s is the shear length, and L_n is the plasma scale (radial) length. The equation for D is given in Ref. (1) for diffusion arising from the enhanced drift wave fluctuations themselves. A detailed derivation utilizing the properties of orbital stochasticity has been given recently.[5] The last term on the right-hand side of Eq. (1) assures that the adiabatic response, $f_e = \frac{e\phi}{T_e} F_e$, is unaffected by diffusion, a consequence of a dynamic constraint peculiar to the $\underline{E} \times \underline{B}$ radial motion.[6] This term would not appear if the diffusion were a result of collisions, although for the small values of D appropriate to that case, one can show that this term has an insignificant effect. In general D is a function of $v_\parallel$, with the dependence varying according to the underlying cause of the diffusion. The correlation frequency,

$$\omega_c = [(k'_\parallel v_e)^2 \frac{D}{3}]^{1/3}, \qquad (2)$$

gives the time the particles remain in resonance with the wave. In the earlier work[1], this diffusion operator was replaced by the correlation frequency, in which case Eq. (1) becomes

$$\left(\frac{\partial}{\partial t} + ik_{\parallel}' x v_{\parallel} + \omega_c\right) f_e$$

$$= -i \frac{e}{T_e} F_e \{\omega_* [1 + \eta_e (\frac{v_{\parallel}^2}{v_e^2} - \frac{1}{2})] - k_{\parallel}' x v_{\parallel} + i\omega_c\} \phi \ . \qquad (3)$$

We will refer to this as the Krook approximation.

The finite-gyroradius ion response is calculated from linear theory:

$$\left(\frac{\partial}{\partial t} + ik_{\parallel}' x\ v_{\parallel}\right)\ h_i = -i\frac{e}{T_e} F_i \Big(\{\omega_* [1 + \eta_i (\frac{v_{\parallel}^2}{v_i^2} - \frac{1}{2})]$$

$$+ \tau\ k_{\parallel}' x\ v_{\parallel}\} [\Gamma_0 + (\Gamma_0 - \Gamma_1)\rho_i^2 \frac{\partial^2}{\partial x^2}]$$

$$-\eta_i \omega_* \{b_y(\Gamma_0 - \Gamma_1) - [\Gamma_0 - 2b_y(\Gamma_0 - \Gamma_1)]\rho_i^2 \frac{\partial^2}{\partial x^2}\}\Big)\phi . \qquad (4)$$

We calculate the distribution

$$h_i = g_i - \frac{e}{T_i} F_i [\Gamma_0 + (\Gamma_0 - \Gamma_1)\rho_i^2 \frac{\partial^2}{\partial x^2}]\phi ,$$

where $g_i \equiv f_i + \frac{e}{T_i} F_i \phi$ is the nonadiabatic response, because, for numerical computation, it is advantageous to have no time derivatives among the potential driving terms [see right-hand side of Eq. (4)]. In the limit of zero ion gyroradius, h_i reduces to the total ion response f_i. The notation in Eq. (4) is

$$F_i = \frac{n_o}{\sqrt{\pi} v_i} e^{-v_\parallel^2/v_i^2}, \quad \eta_i = \frac{d\ (\ln T_i)}{d\ (\ln n_o)}, \quad \rho_i = \frac{v_i}{\sqrt{2}\Omega_i}, \quad v_i = \sqrt{\frac{2T_i}{m_i}},$$

$$\tau = \frac{T_e}{T_i}, \quad \Gamma_n = \exp(-b_y) I_n(b_y), \quad b_y = (k_y \rho_i)^2 .$$

The time-evolution drift instability computer code TEDIT uses an implicit-iterative scheme to advance the electron and ion kinetic equations in time, with ϕ being calculated from the quasi-neutrality condition

$$[1 - \Gamma_0 - (\Gamma_0 - \Gamma_1)\rho_i^2 \frac{\partial^2}{\partial x^2}]\phi = \frac{T_i}{e n_0} \int_{-\infty}^{\infty} dv_\parallel (h_i - f_e) . \qquad (5)$$

Equations (1) and (4) are advanced in time until

$$\omega(x,t) = \frac{i}{\phi(x,t)} \frac{\partial \phi(x,t)}{\partial t}$$

becomes independent of both x and t, indicating that an eigenmode of frequency ω has been established. For a given set of physical parameters, TEDIT yields the most unstable eigenmode.

III. NUMERICAL RESULTS AND INTERPRETATION

In Fig. 1 we show the growth rate as a function of the diffusion parameter ω_c for various poloidal wave numbers. Three sets of results are shown: (1) those obtained using the Krook-type approximation, (2) those obtained from a better approximate treatment of the diffusion operator in a shooting code,[7] and (3) those obtained from TEDIT using the full diffusion operator.

The Krook approximation curves may be obtained either from a shooting code of the type used in Ref. 1 or from TEDIT using Eq. (3); results from the two methods agree extremely well. Use of the approximate diffusion operator is an attempt to include diffusion in a shooting code and is shown in order to corroborate the TEDIT results; in these results, D was assumed to be independent of $v_\parallel$.

The noteworthy features are (1) higher growth rate in the case of the full diffusion operator and (2) the significantly larger diffusion required to stabilize the mode. Both of these phenomena can be understood from the large ω_c asymptotic limit of the diffusive electron response outlined in the Appendix and displayed in Fig. 2. In the Appendix we show that both the Krook approximation and diffusion lead to a response of the same qualitative form in the limits $\omega\tau_c < 1$ and $x_c/x_T < 1$ ($x_c \cong \omega_c/k'_\parallel v_e$, x_T = mode "length") at both small x ($x < x_c$) and large x ($x > x_c$). The difference amounts to a numerical factor in the small x response. Since this region plays the dominant role in determining stability, we use this limit to interpret the numerical results. Accordingly, assuming that the shear (or ion) damping γ_i is constant at constant frequency (here taken as the local dispersion relation frequency for the universal mode) and that the electron response is proportional to τ_c, the correlation time, we can approximate the growth rate at large ω_c by

$$\gamma \simeq \frac{\alpha}{\omega_c} - \gamma_i \ , \tag{6}$$

whereas evaluation of the diffusive electron response (Appendix) gives

$$\gamma \simeq \frac{2.82\alpha}{\omega_c} - \gamma_i \ . \tag{7}$$

By evaluating α from two points on the Krook-type curve in Fig. 2 and translating the results to our diffusion operator curve, we see good agreement. The dots indicate γ as calculated using the scalings in Eqs. (6) and (7).

Of course other effects come into play. The $v_\parallel$ dependence of the correlation time in the full diffusion model (upon integration over all particles) affects the magnitude of the net dissipation. Also, the wave frequency is dependent on ω_c and decreases as $\omega_c \to 0$. In fact, as $\omega_c \to \infty$, the wave frequency asymptotes to the local disperion relation solution, ω_∞, indicating that the diffusion operator has, in effect, destroyed the cold electron response near $x = 0$. Still another effect is a modification of ϕ at very large ω_c.

We can further observe the radial perturbed eigenfunctions $\phi(x)$. In both the small ω_c region [that is, where $\gamma(\omega_c)$ is increasing for both the Krook-type and diffusive cases, Fig. 3a] and in the large ω_c regime (Fig. 3b), the eigenmodes are very similar, whether calculated by the Krook-type approximation or by the diffusion operator. [For large ω_c, we compare results at $\omega_c(\text{diffusion}) = 2.5\ \omega_c(\text{Krook})$, with the numerical factor sufficiently close to 2.8 to cause a negligible difference in ϕ].

Note that x_i ($\cong \omega/k_\parallel' v_i$) has moved well into the body of the eigenfunction and there is not a clear outgoing wave region. This is a consequence of large $k_y\rho_i$, where $x_i \to x_T$. Nonetheless, the electron growth and ion damping regions are separated spatially, and the eigenfunction apparently convects the energy from electrons to ions at the conventional shear damping rate.

A. Velocity-dependent diffusion coefficient

As derived earlier,[1] D (for electrostatic perturbations) is not constant but is proportional to $|v_\parallel|^{-1}$ at large $v_\parallel$, and at small $v_\parallel$ the turbulent diffusion approaches zero because the electron resonances are beyond the eigenfunction. For use in Eq. (1), we, therefore, take D to be of the form

$$D = D_c + D_o \frac{v_e}{|v_\parallel|} \exp\left(-\frac{v_c^2}{v_\parallel^2}\right) . \tag{8}$$

Here, D_c represents a residual diffusion on the order of magnitude of collisional diffusion, v_c represents the cutoff velocity below which turbulent diffusion $\to 0$, and D_o is determined by the amplitude of ϕ [see Eq. (2)]. The parameter v_c/v_e depends on details of the large x behavior of the perturbed ϕ and is treated here as a parameter on the order of x_c/x_T. Results showing the growth rate of the nonlinear universal mode (Fig. 4) reveal several important points:

(1) The residual diffusion arising from collisions is sufficient to destabilize the universal mode in the absence of wave-induced stochasticity, thereby eliminating the need to argue for a threshold level of stochasticity from other sources.

(2) The saturation level of diffusion appears to be strongly dependent on the details of wave absorption at large x, here represented by the parameter v_c. The reason for this is because f_e, which peaks

strongly about $v_\parallel \approx 0$, has a fine structure from wave-particle resonances near $v_\parallel = 0$ (and large x). Unlike the D = constant case, this fine structure (on the order of $10^{-3}v_e$) is not smoothed out by spatial diffusion. It does suggest that velocity-space diffusion from Coulomb collisions could have significant influence on determining the actual value of saturation. Moreover, it also suggests that an outgoing wave boundary condition would not predict saturation levels of ϕ (or D).

(3) The numerical differences observed upon using a proper $D(v_\parallel)$ are as significant as those seen by changing from a Krook to diffusion operator. This implies that it is the $v_\parallel$ dependence of the correlation time, not diffusion, that is causing the numerical differences.

E. Electron temperature gradient

The results displaying growth rate for various temperature gradients are shown in Fig. 5. As expected, η_e has a strong stabilizing influence on the mode, eliminating the unstable region, for $b_y = 4$, at $\sim \eta_e = 2$. This is reminiscent of the simple argument that the electron dissipation [see Eq. (1)] becomes positive for $\eta_e = 2$ if one puts $(v_\parallel/v_e)^2 = (\omega/k_\parallel v_e) \ll 1$. Actually, the η_e scaling is somewhat weaker than this because the resonance broadening brings the larger $v_\parallel$ particles into play. Saturation at $\eta_e = 2$ comes about because the electron dissipation is sufficiently small, although still negative, that it can be offset by shear damping. To see this in more detail, note that the electron dissipation can be written (see Appendix) as

$$\gamma_e \propto \int_{-\infty}^{+\infty} dv_\parallel F_e(v_\parallel) \int_0^\infty d\tau \exp\left[i(\omega - k'_\parallel v_\parallel x)\tau - \frac{1}{3}(k'_\parallel v_\parallel)^2 D\tau^3\right]$$

$$\times \{\omega - \omega_*[1 + \eta_e(\frac{v_\parallel^2}{v_e^2} - \frac{1}{2})]\} \ . \qquad (9)$$

This can be evaluated for $x < x_c$ from the integrals $I^{(0)}$ and $I^{(2)}$ given in the Appendix. The result is

$$\gamma_e \propto [\omega - \omega_*(1 - \eta_e/3)]\ \tau_c \ , \qquad (10)$$

so that the electron dissipation remains negative up to $\eta_e = 3$. Thus, for $b_y >> 1$ when $\omega << \omega_*$, the ω_c required to saturate the mode should, according to Eq. (10), scale as $1 - \eta_e/3$. This scaling is illustrated, and roughly confirmed, in the following table.

Temperature gradient scaling of saturation points. Saturation values of ω_c from Fig. (5) are compared to various scalings of the η_e dependence. The observed scaling is clearly weaker than $(1 - \eta_e/2)$, with the inferred coefficient of η_e lying between 1/3 and 1/4.

η_e	$3.2(1 - \eta_e/2)$	$3.2(1 - \eta_e/3)$	$3.2(1 - \eta_e/4)$	ω_c^{SAT}/ω_*
0	3.2	3.2	3.2	3.2
1	1.6	2.1	2.4	2.7
1.8	0.32	1.3	1.8	1.6

ACKNOWLEDGEMENTS

The authors would like to thank Dr. J. C. Whitson for his help and in providing us with some of his unpublished results. We would also like to acknowledge useful discussions with Profs. J. Denavit of Northwestern University, J. P. Freidberg of Massachusetts Institute of Technology, and D. Ross and D. Hitchcock of Institute for Fusion Studies.

APPENDIX

Asymptotic Evaluation of Diffusive Electron Response

The electron response can be written as $f_e = \frac{e\phi}{T_e} F_e + h_e$, where h_e satisfies [see Eq. (1)],

$$\left[-i(\omega - k_\parallel' v_\parallel x) - D\frac{\partial^2}{\partial x^2}\right] h_e$$

$$= i\{\omega - \omega_*\left[1 + \eta_e\left(\frac{v_\parallel^2}{v_e^2} - \frac{1}{2}\right)\right]\frac{eF_e}{T_e}\}\ \phi(x) \ . \qquad (A.1)$$

This is easily solved by transform methods to give

$$h_e(x, v_\parallel) = \int_0^\infty d\tau \int_{-\infty}^{+\infty} dx' \exp\left[i(\omega - k_\parallel' v_\parallel x)\tau - \frac{1}{3}(k_\parallel' v_\parallel)^2 D\tau^3\right]$$

$$\frac{1}{\sqrt{4\pi D\tau}} \exp\left(-\frac{(x - x' - iDk_\parallel' v_\parallel \tau^2)^2}{4D\tau}\right)\phi(x')$$

$$\times\ i\{\omega - \omega_*\left[1 + \eta_e\left(\frac{v_\parallel^2}{v_e^2} - \frac{1}{2}\right)\right]\}\frac{eF_e}{T_e} \ . \qquad (A.2)$$

The nonadiabatic electron density fluctuation is then

$$\tilde{n}_e^{NA}(x) = \int dv_\parallel \frac{e}{T_e}\, i\{\omega - \omega_*\left[1 + \eta_e\left(\frac{v_\parallel^2}{v_e^2} - \frac{1}{2}\right)\right]\}\ F_e$$

$$\times \int_0^\infty d\tau \int_{-\infty}^{+\infty} dx' \exp\left[i(\omega - k_\parallel' v_\parallel x)\tau - \frac{1}{3}(k_\parallel' v_\parallel)^2 D\tau^3\right]$$

$$\times \frac{1}{\sqrt{4\pi D\tau}} \exp\left[-\frac{(x - x' - iDk_\parallel' v_\parallel \tau^2)^2}{4D\tau}\right]\phi(x'). \qquad (A.3)$$

This complicated integral operator is the analytic manifestation of the full electron response, Eq. (1). The transcendental dependence on D makes it very difficult to apply in shooting codes [particularly when a realistic $D = D(v_\parallel)$ dependence is allowed], over the full range of D and x values of interest. At the same time, one's ability to make analytic predictions is somewhat limited. Fortuitously, in the region where the most unstable modes saturate (from which the turbulent diffusion coefficient is computed), some asymptotic expansions can be made, which give a reasonable accounting of the numerical observations in the body of this paper. This regime is characterized by $k_y\rho_i > 1$ so that $\omega << \omega_*$, and since $\omega_*\tau_c > 1 (\tau_c = \omega_c^{-1})$, $\omega\tau_c << 1$ is typical. Furthermore, $x_c \equiv 1/k_\parallel' v_e \tau_c$ is less than $x_T \equiv |d\ln\phi/dx|^{-1}$, although this is not a strong inequality.

First consider the integral operator

$$O(x;v_\parallel,\tau) = \int dx' G(x,x';v_\parallel,\tau)\phi(x'), \qquad (A.4)$$

where G is the kernel,

$$G(x,x';v_\parallel,\tau) = \frac{1}{\sqrt{4\pi D\tau}} \exp\left[i(\omega - k_\parallel' v_\parallel x)\tau - \frac{1}{3}(k_\parallel' v_\parallel)^2 D\tau^3 - \frac{(x - x' - iDk_\parallel' v_\parallel \tau^2)^2}{4D\tau}\right]. \qquad (A.5)$$

Note that G is a peaked function of $x - x'$ with width x_c, whereas x_T is the basic scale of ϕ. Thus, for $x_c/x_T < 1$, $\phi(x')$ can be Taylor expanded about $x' = x$,

$$\Theta(x;v_{\parallel},\tau) = \int d\delta x\, G(x,\, x+\delta x;v_{\parallel},\tau)\left[\phi(x) + \delta x\frac{d\phi}{dx} + \frac{1}{2}\delta x^2\frac{d^2\phi}{dx^2} + \ldots\right] ,$$

and doing the integral yields

$$\Theta(x;v_{\parallel},\tau) = C_{k,\omega}(x;v_{\parallel},\tau)\{\phi(x) - iDk'_{\parallel}v_{\parallel}\tau^2\frac{d\phi}{dx}$$

$$+ \frac{1}{2}D\tau\left[2-(k'_{\parallel}v_{\parallel})^2D\tau^3\right]\frac{d^2\phi}{dx^2} + \ldots\} , \qquad (A.6)$$

where

$$C_{k,\omega}(x;v_{\parallel},\tau) = \exp\left[i(\omega - k'_{\parallel}v_{\parallel}x)\tau - \frac{1}{3}(k'_{\parallel}v_{\parallel})^2D\tau^3\right] .$$

With some rearranging, Eq. (A.6) can be written as

$$O(x;v_{\parallel},\tau) = C_{k,\omega}(x;v_{\parallel},\tau)\phi(x) + \frac{d}{dx}\left[D\tau C_{k,\omega}(x;v_{\parallel},\tau)\frac{d}{dx}\phi(x)\right]$$

$$- \frac{1}{2}\,(Dk'_{\parallel}v_{\parallel}\tau^2)^2C_{k,\omega}(x;v_{\parallel},\tau)\,\frac{d^2}{dx^2}\,\phi(x) + \ldots . \qquad (A.7)$$

Equation (A.7) illustrates one of the basic difficulties in approximating the original integral operator (A.4) by some nth order differential operator. While the original operator (A.4) was self-adjoint (G is a symmetric kernel), Eq. (A.7), to the order written, obviously is not. We, therefore, argue that the last term in Eq. (A.7), although formally of order $(x_c/x_T)^2$ like the second term,

should actually be combined with some of the $(x_c/x_T)^4$ terms to make a self-adjoint operator to that order.

For present purposes of interpreting the numerical results, we regard $\tilde{n}_e^{NA}$ as the dissipation response and retain simply the leading order term of Eq. (A.7). The response is then reduced to evaluating integrals of the form

$$I^{(n)}(x) = \int_0^\infty d\tau \int_{-\infty}^{+\infty} dv_\parallel \frac{\exp(-v_\parallel{}^2/v_e{}^2)}{\sqrt{\pi} v_e} \; C_{k,\omega}(x; v_\parallel, \tau) v_\parallel{}^n. \qquad (A.8)$$

For example, after doing the $v_\parallel$ integrals, $I^{(0)}$ becomes

$$I^{(0)} = \tau_c \int_0^\infty ds \; \exp\left[i\omega\tau_c s - \frac{1}{4}\left(\frac{x}{x_c}\right)^2 \frac{s^2}{1+s^3}\right] / (1+s^3)^{1/2} .$$

For large x/x_c, the asymptotic behavior of $I^{(0)}$ is

$$I^{(0)} \sim \tau_c \sqrt{\pi} \frac{x_c}{x} \sim \frac{\sqrt{\pi}}{k_\parallel' v_e x} ,$$

which is independent of D and corresponds to the diffusionless response. For small x/x_c, $I^{(0)} \equiv \tau_c \int_0^\infty ds \; (1 + s^3)^{-1/2} \exp(i\omega\tau_c s)$, which is still transcendental. For $\omega\tau_c \lesssim 1$, however, as happens in practice, the integral can be evaluated in terms of beta functions,

$$I^{(0)} \sim \tau_c \frac{1}{3} B\left(\frac{1}{3}, \frac{1}{6}\right).$$

Note that as $x \to 0$, $I^{(0)}$ has a singular dependence on D, $\tau_c \propto D^{-1/3}$, underscoring the sensitivity of the drift wave to small amounts of radial diffusion.

For evaluating various further approximations and other purposes, it will be convenient to have interpolation formulas for the $I^{(n)}$ obtained by matching the large and small x behavior. These are written in terms of interpolation functions, $g_n(x/x_c)$, normalized such that $g_n(0) = 1$. Proceeding as above, one obtains

$$I^{(0)} = 2.80\tau_c g_0\left(\frac{x}{x_c}\right) \qquad ;g_0(y) = (1 + 1.58y)^{-1}$$

$$I^{(2)} = 0.47\tau_c\, g_2\left(\frac{x}{x_c}\right) \qquad ;g_2(y) = (1 + y^4)^{-1}$$

$$I^{(1)} = \frac{-i}{k_\parallel' x v_e} \frac{0.29x^2}{x_c^2} g_1\left(\frac{x}{x_c}\right) \quad ;g_1(y) = (1 + 0.29y^2)^{-1}$$

$$I^{(3)} = \frac{-i}{k_\parallel' x v_e} \frac{0.24x^2}{x_c^2} g_3\left(\frac{x}{x_c}\right) \quad ;g_2(y) = (1 + 0.48y^2)^{-1}.$$

The Krook approximation uses

$$C_{k,\omega}(x;v_\parallel,\tau) = \exp[(i(\omega - k_\parallel' v_\parallel x)\tau - \omega_c\tau]$$

which leads to $I^{(n)}$ integrals expressed in terms of Z functions. For example, under this approximation, $I^{(0)}$ goes over to

$$I_Z^{(0)}(x) = \frac{-i}{k_\parallel' v_e |x|} Z\left(\frac{x_e + ix_c}{|x|}\right) . \qquad (A.9)$$

Since $x_c >> x_e$ at saturation, the asymptotic limits of the approximation are

$$I_Z^{(0)}(x) \cong \begin{cases} \tau_c & |x| < x_c \\ \dfrac{\sqrt{\pi}}{k_\parallel' v_e |x|} & |x| > x_c \end{cases} .$$

Thus, in spite of its poor justification, the Z function approximation of the resonance function has the correct qualitative features at both large and small x. By multiplying x_c by a numerical factor, the correct asymptotic behavior can be recovered so that

$$I^{(0)} = \frac{-i}{k_\parallel' v_e |x|} Z\left(\frac{x_e + i\ 0.36 x_c}{|x|}\right) \qquad \text{(A.10)}$$

can be regarded as an alternate interpolation formula.

REFERENCES

1. S. P. Hirshman and K. Molvig, Phys. Rev. Lett. 42, 648 (1979).
2. K. Molvig, S. P. Hirshman, and J. C. Whitson, Phys. Rev. Lett. 43, 582 (1979).
3. G. M. Zaslavskii and B. V. Chirikov, Sov. Phys. Usp. 14, 549 (1972)[Van. fiz. nauk. 105, 3 (1971)].
4. C. O. Beasley, Jr., W. I. van Rij, J. Denavit, and J. E. McCune, Bull. Am. Phys. Soc. 24, 1039 (1979).
5. K. Molvig, J. P. Freidberg, R. Potok, S. P. Hirshman, and J. C. Whitson, to be published.
6. D. Thayer and K. Molvig, (to be published); T. H. Dupree and D. J. Tetrault, Phys. Fluids 21, 425 (1978).
7. J. C. Whitson (Oak Ridge National Laboratory), private communication, 1981.

FIGURE CAPTIONS

FIG. 1. Growth rate (obtained numerically) vs diffusion parameter, ω_c, for various models and values of $b_y = k_y^2 \rho_i^2$. The dashed curves indicate the results of the Krook approximation, Eq. (3), as used in Ref. 1. The full diffusion operator results are shown in solid lines and indicate qualitatively similar behavior with some quantitative differences.

FIG. 2. Analytic explanation of change in growth rates. Two representative curves for the Krook approximation and full diffusion operator, obtained from the numerical code, are shown as solid lines. The attempt to fit these curves with asymptotic analytic expressions is indicated by the dots. The difference amounts simply to the adjustment of the Krook model coefficient by a numerical factor.

FIG. 3. Real part of the radial eigenfunction.

FIG. 3a. Near destabilization.

FIG. 3b. Near saturation.

FIG. 4. Growth rate vs the correlation frequency, ω_c, for the $v_\parallel$ dependence of D as expressed by Eq. (8), showing dependence on cutoff parameter v_c. (ω_c is determined from D_o, the turbulent part of diffusion coefficient). Results for constant D are shown for comparison.

FIG. 5. Growth rate vs the correlation frequency for several values of the temperature gradient parameter, $n_e = \frac{d\,(\ln T_e)}{d\,(\ln n_o)}$. These results use the constant D model.

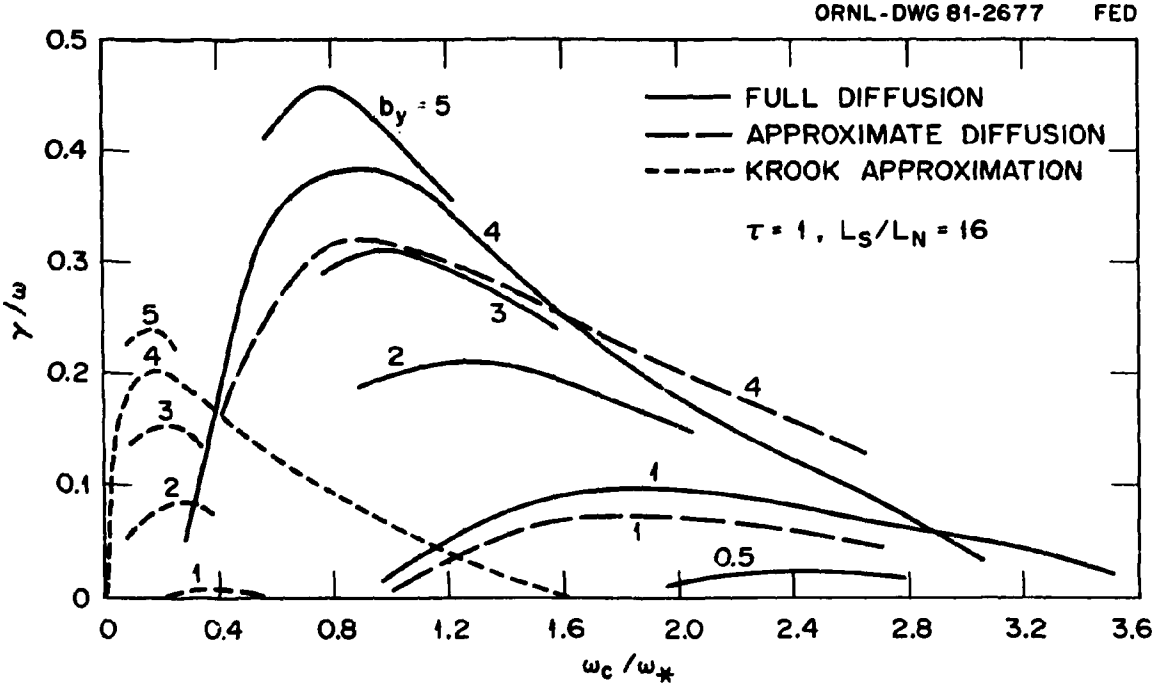
ORNL-DWG 81-2677 FED
FULL DIFFUSION
APPROXIMATE DIFFUSION
KROOK APPROXIMATION
τ = 1, L_S/L_N = 16
b_y = 5
γ/ω
ω_c/ω_*
0.5
0.4
0.3
0.2
0.1
0
0.4
0.8
1.2
1.6
2.0
2.4
2.8
3.2
3.6

Fig. 1

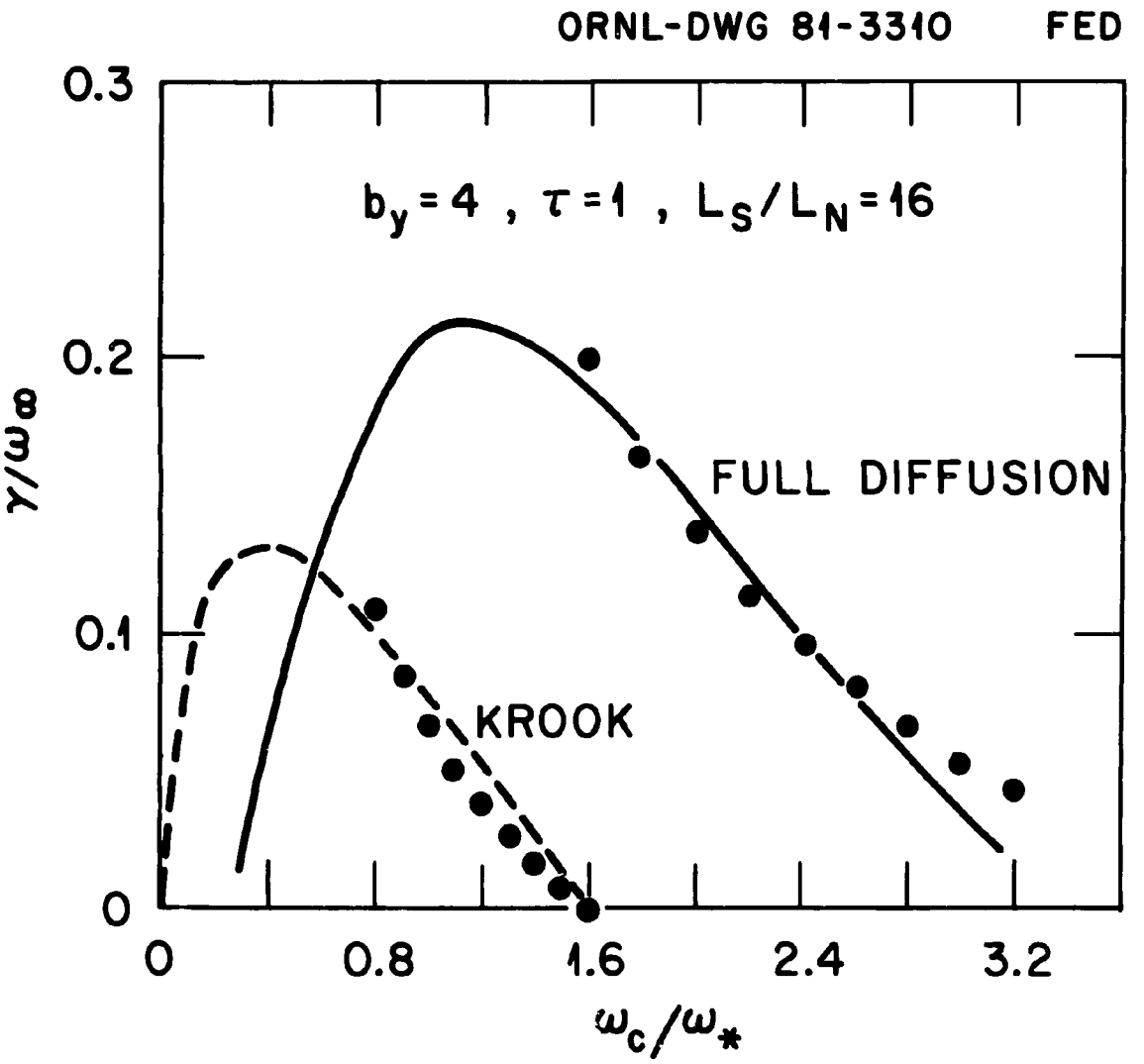
ORNL-DWG 81-3310 FED
0.3
0.2
0.1
0
$b_y = 4$, $\tau = 1$, $L_S/L_N = 16$
γ/ω_B
FULL DIFFUSION
KROOK
0
0.8
1.6
2.4
3.2
ω_c/ω_*

Fig. 2

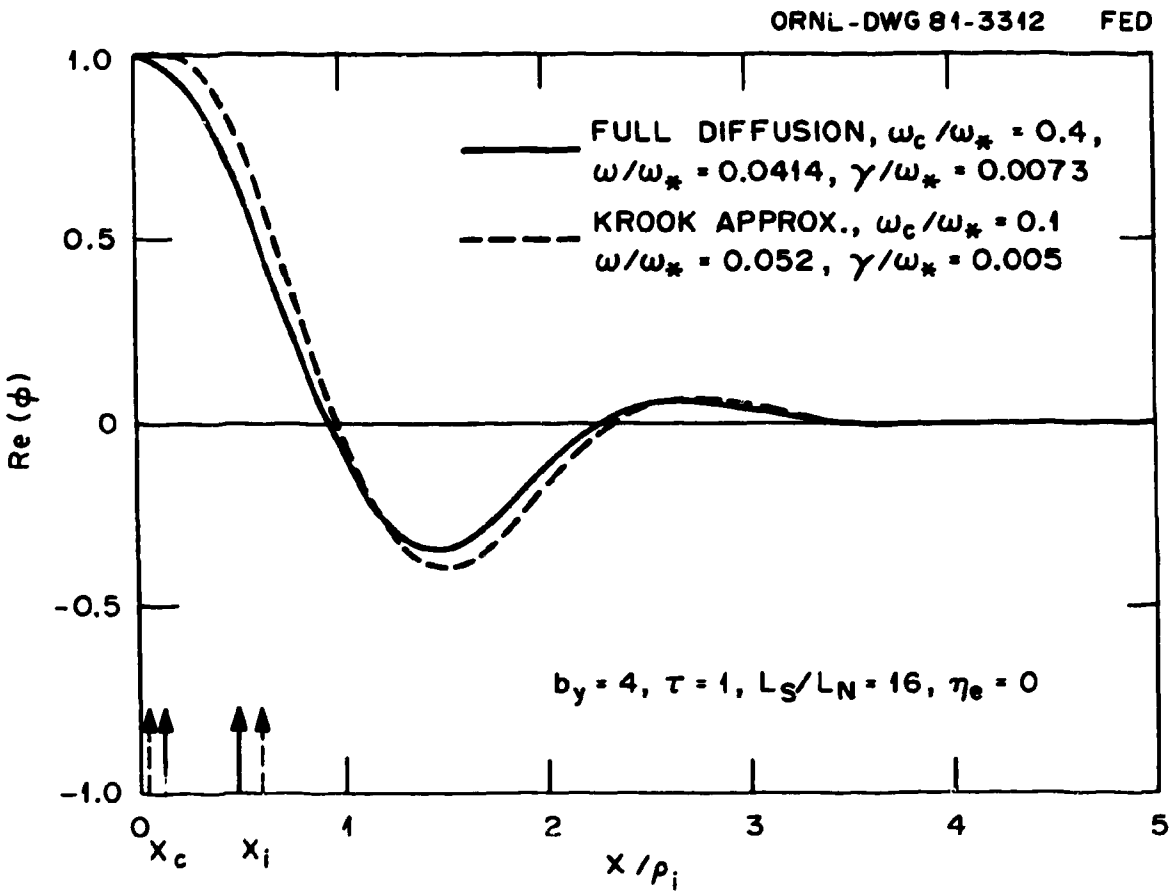
ORNL-DWG 81-3312 FED
FULL DIFFUSION, $\omega_c/\omega_* = 0.4$, $\omega/\omega_* = 0.0414$, $\gamma/\omega_* = 0.0073$
KROOK APPROX., $\omega_c/\omega_* = 0.1$ $\omega/\omega_* = 0.052$, $\gamma/\omega_* = 0.005$
$b_y = 4$, $\tau = 1$, $L_S/L_N = 16$, $\eta_e = 0$
Re (ϕ)
1.0
0.5
0
-0.5
-1.0
0
x_c
x_i
1
2
3
4
5
x/ρ_i

Fig. 3a

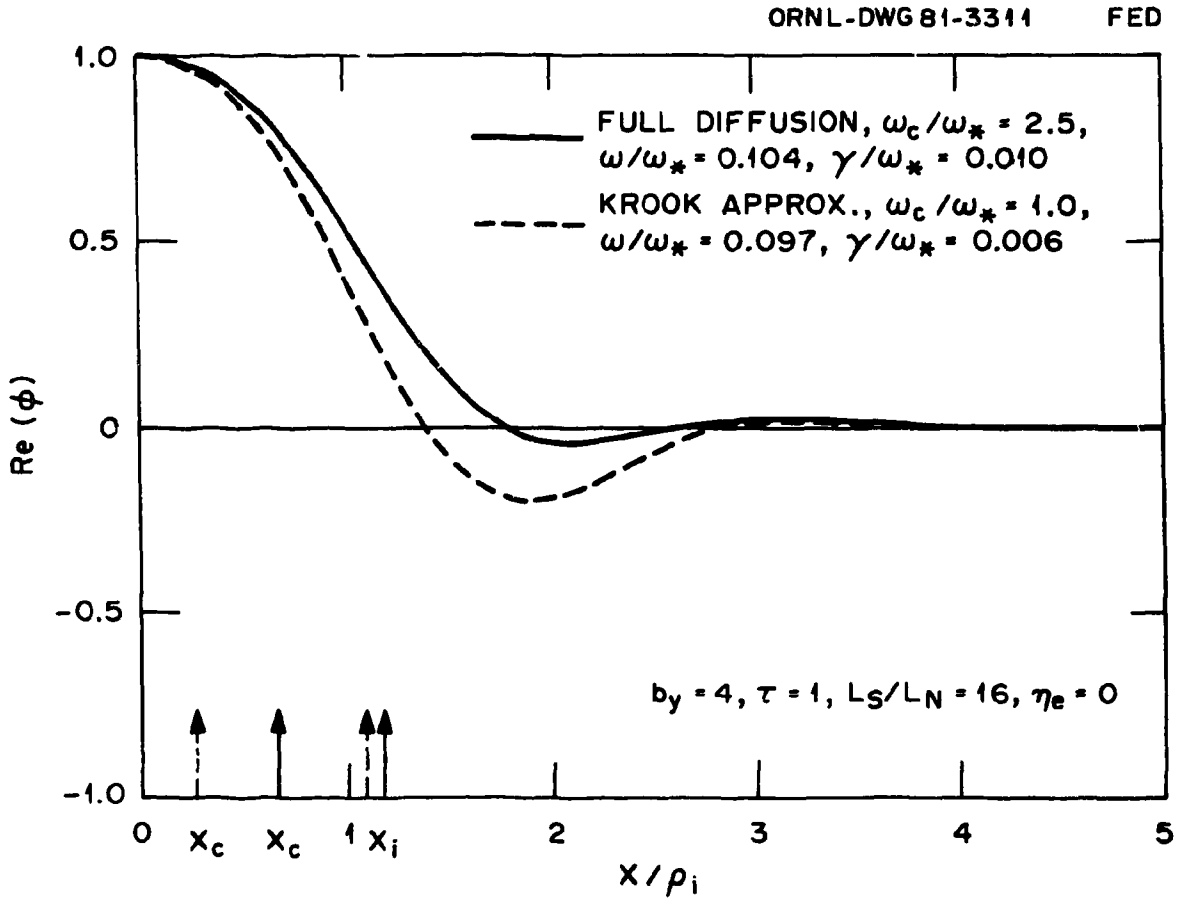
ORNL-DWG 81-3311 FED
1.0
0.5
0
-0.5
-1.0
Re (φ)
FULL DIFFUSION, ω_c/ω_* = 2.5,
ω/ω_* = 0.104, γ/ω_* = 0.010
KROOK APPROX., ω_c/ω_* = 1.0,
ω/ω_* = 0.097, γ/ω_* = 0.006
b_y = 4, τ = 1, L_S/L_N = 16, η_e = 0
0
x_c
x_c
1
x_i
2
3
4
5
X/ρ_i

Fig. 3b

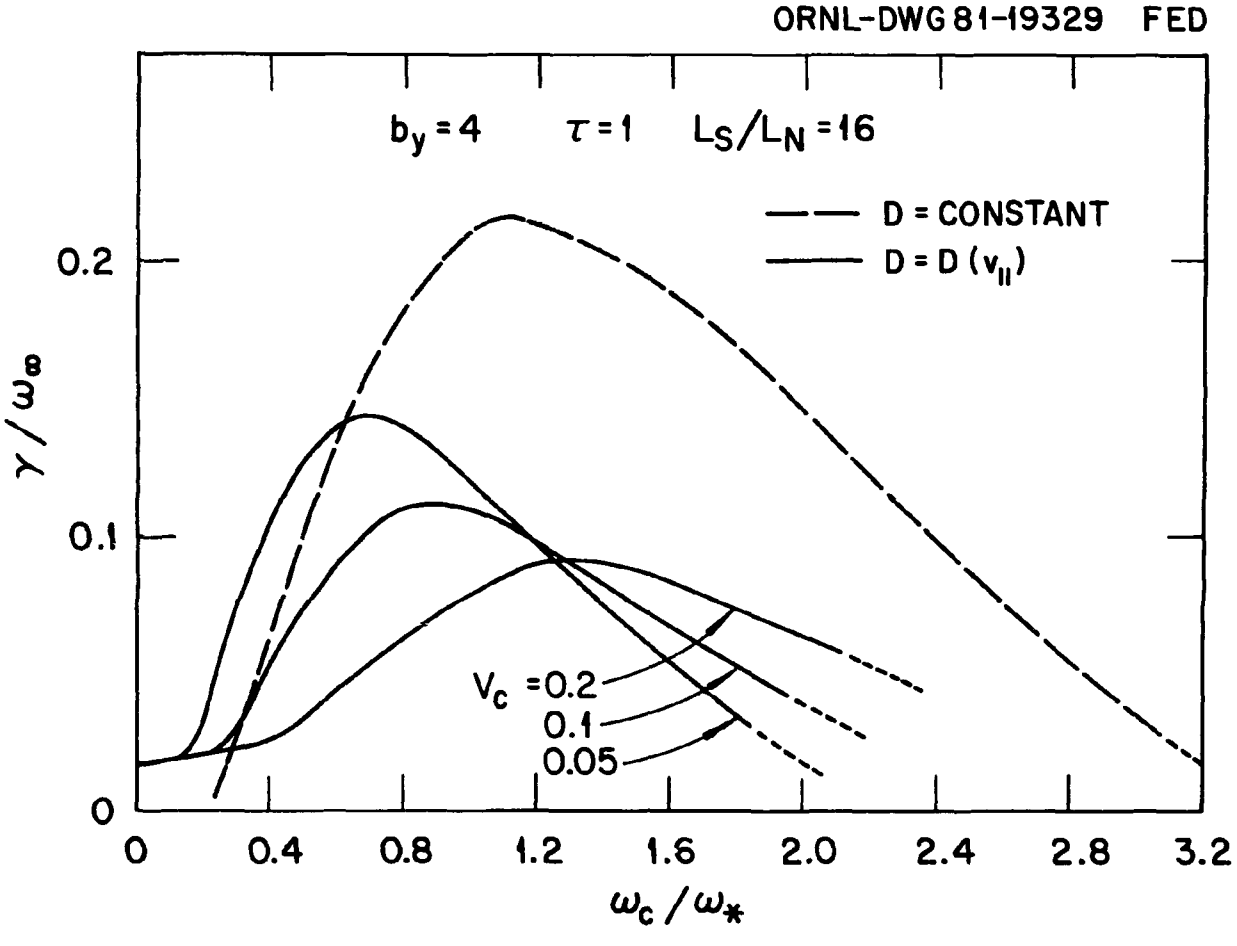
ORNL-DWG 81-19329 FED
$b_y = 4$ $\tau = 1$ $L_S/L_N = 16$
D = CONSTANT
D = D ($v_{||}$)
V_c =0.2
0.1
0.05
γ / ω_*
ω_c / ω_*
0
0.1
0.2
0.4
0.8
1.2
1.6
2.0
2.4
2.8
3.2

Fig. 4

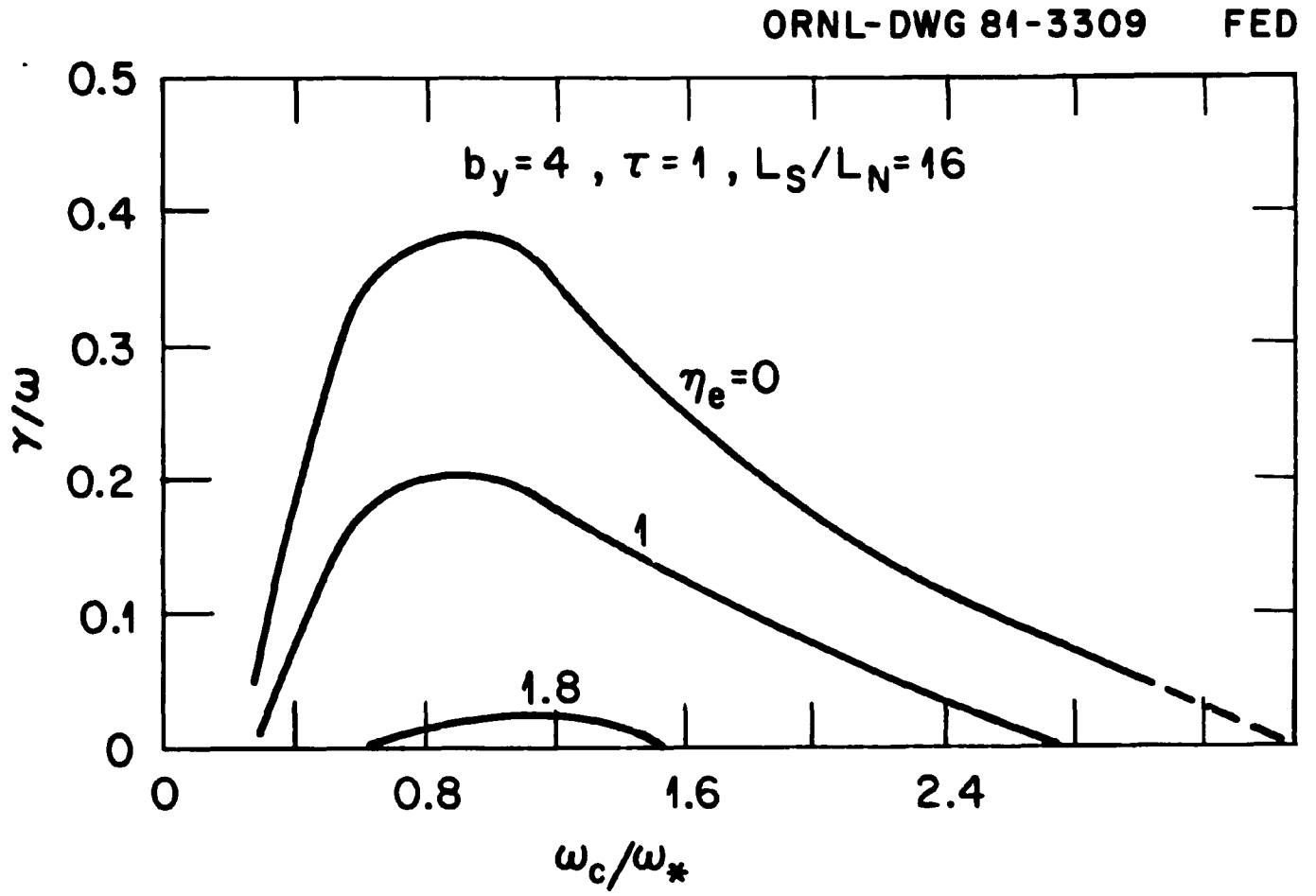
ORNL-DWG 81-3309 FED
$b_y = 4$, $\tau = 1$, $L_S/L_N = 16$
$\eta_e = 0$
1
1.8
γ/ω
ω_c/ω_*
0.5
0.4
0.3
0.2
0.1
0
0.8
1.6
2.4

Fig. 5